# Chaotic motions of a tethered satellite system in circular orbit

**D P Jin[1], Z J PANG, H Wen and B S Yu**

State Key Laboratory of Mechanics and Control of Mechanical Structures, Nanjing University of Aeronautics and Astronautics, 29 Yudao Street, Nanjing 210016, China
[1] E-mail: jindp@nuaa.edu.cn

**Abstract.** This paper studies the chaotic motions of a tethered satellite system by utilizing a ground-based experimental system. Based on dynamics similarity principle, a dynamical equivalent model between the on-orbit tethered satellite and its ground physical model is obtained. As a result, the space dynamics environment of the tethered satellite can be simulated via the thrust forces and the torque of a momentum wheel on the satellite simulator. The numerical results of the on-orbit tethered satellite show the chaotic motions of the attitude motion of mother satellite. The experiment shows that the torque of momentum wheel as a negative damping is able to suppress the chaotic motion.

## 1. Introduction

There are different varieties of nonlinear dynamic phenomena in tethered satellite systems such as tumbling [1], internal resonances [2], chaotic motions [3,4], and the like [5]. It is necessary to reveal the nonlinear dynamics of a tethered satellite system for accurate control [6].

It is clear that a two-body tethered satellite system exhibits chaotic motions [7], especially for that of large orbit eccentricity [8]. Steiner investigated the transient chaos of a tethered satellite by finite-element method [9]. Misra et al. found that the three-dimensional coupled pitch and roll motions of a tethered spacecraft will be chaotic whatever in elliptic orbit or in circular orbit [10]. Many on-orbit missions of tethered satellite had been carried out [11], since the first space flying in 1966 for creating artificial gravity by spinning two spacecrafts connected by a tether. At the same time, various types of experiment setup for the dynamics and control of tether system in laboratory scale have been constructed. For example, Kojima et al. proposed a slope-adjustable turntable to simulate the in-plane motion of a tethered satellite system in elliptic orbit, making use of a piece of dry ice in an attempt to reduce the friction between turntable and satellite [12[. However, the nonlinear dynamics and control of tethered satellite systems via ground-based experiment in consideration of the microgravity and the Coriolis force still needs to strengthen further.

This paper studies the chaotic motion of a tethered satellite system with the attitude motion of mother satellite. A dynamics similarity between the on-orbit tethered satellite and its physical model is presented.

## 2. Chaotic motions of tethered satellite system

Consider an in-plane tethered satellite system moved in an unperturbed Kepler circular orbit, as shown in figure 1. The mother satellite is treated as a rigid body of mass *M*, and the subsatellite is envisioned to be a point of mass *m* that is attached to the mother satellite through an inelastic massless tether of length *l* at the joint point of the offset distance $\rho<<l$ to the mass center of the mother satellite. It is assumed that the mass of the mother satellite is much greater than that of the subsatellite, and the center of mass of the system coincides with that of the mother satellite. The earth-centered inertial frame is denoted by *O-XYZ*, the origin of which is located at the center of the Earth. $I_x$, $I_y$ and $I_z$ are the principal moments of inertia of the mother satellite expressed in its body frame.

By an application of Lagrange's equations, the dynamic equation reads

$$\begin{cases} \ddot{\theta} = -3\sin\theta\cos\theta \\ \quad -\beta_1[(\dot{\alpha}^2 + 2\dot{\alpha})\sin(\theta-\alpha) + 3\cos\alpha\sin\theta - \beta_0\sin\alpha\cos\alpha\cos(\theta-\alpha)] \\ \ddot{\alpha} = -\beta_0\sin\alpha\cos\alpha + \beta_2[\dot{\theta}^2 + 2\dot{\theta} + 3\cos^2\theta]\sin(\theta-\alpha) \end{cases} \tag{1}$$

with $\beta_0 = 3(I_y - I_x)/I_z$, $\beta_1 = \rho/l$, and $\beta_2 = M\rho l/I_z$. The overdot denotes the derivative with respect to the true anomaly $\nu$.

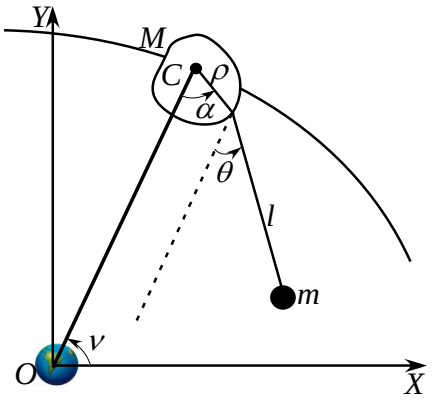


Figure 1. Model of tethered satellite system.

It can be shown that if we regard $\beta_2$ as a perturbation to the attitude motion of mother satellite, the unperturbed system in equation (1) becomes [4]

$$\ddot{\alpha} = -\beta_0\sin\alpha\cos\alpha \tag{2}$$

with the Hamiltonian $h_2 = \dot{\alpha}^2 + \beta_0\sin^2\alpha$, so that the attitude motion is divided into two regions by the separatrix of the energy $h_2 = \beta_0$. In the case of $0 < h_2 < \beta_0$, one has

$$\alpha = \arcsin[k_2\,\mathrm{sn}(\sqrt{\beta_0}\nu, k_2)],\quad \dot{\alpha} = \sqrt{h_2}\,\mathrm{cn}(\sqrt{\beta_0}\nu, k_2),\quad k_2^2 = h_2/\beta_0 \tag{3}$$

which corresponds to an oscillation near the local equilibrium of system. For $h_2 > \beta_0$, it arrives at a tumbling rotation as follows

$$\alpha = \arcsin[\mathrm{sn}(\sqrt{\beta_0}\nu, 1/k_2)],\quad \dot{\alpha} = \sqrt{h_2}\,\mathrm{dn}(\sqrt{h_2}\nu, 1/k_2),\quad k_2^2 = h_2/\beta_0 \tag{4}$$

Note that the solutions corresponding to $h_2 = \beta_0$ form the heteroclinic orbit expressed in the following

$$[\alpha^{\pm}(\nu), \dot{\alpha}^{\pm}(\nu)] = \{\pm\arcsin[\tanh(\sqrt{\beta_0}\nu)],\ \pm\sqrt{\beta_0}\,\mathrm{sech}(\sqrt{\beta_0}\nu)\} \tag{5}$$

which pass through two unstable equilibria of the unperturbed system. The existence of heteroclinic intersections depends on the following Melnikov function

$$M(\tau)=\frac{\beta_2}{\sqrt{\beta_0}}\omega\pi\sum_{i=0}^{9}[ia_i\mathrm{csch}(\frac{i\omega\pi}{2\sqrt{\beta_0}})-ib_i\mathrm{sech}(\frac{i\omega\pi}{2\sqrt{\beta_0}})]\sin(i\omega\tau) \tag{6}$$

where $\omega$, $a_i$, and $b_i$ are the expansion coefficient [4].

The calculation of equation (6) shows that the Melnikov function $M(\tau)$ has simple zeroes if $h_1=\dot{\theta}^2+3\sin^2\theta\neq 0$, this implies there exist the heteroclinic intersection between the stable manifold and the unstable manifold. The global Poincaré maps for $\beta_0=1$, $\beta_1=0.001$, and $\beta_2=0.01$ are shown in figure 2. One can see from figure 2 that the attitude motion becomes chaotic as the disturbance increases gradually. The time histories, the Poincaré mapping, the power spectrum density as well as the largest Lyapunov exponent are given in figure 3 for $(\theta_0,\dot{\theta}_0,\alpha_0,\dot{\alpha}_0)=(0.1,0.52,-\pi/2,0.001)$. As can be seen in figures 3(a) and 3(b), the time evolution exhibits an aperiodic motion. In addition, the continuous power spectrum density and the positive largest Lyapunov exponent indicate also the chaotic behavior as shown in figure 3(c) and 3(d).

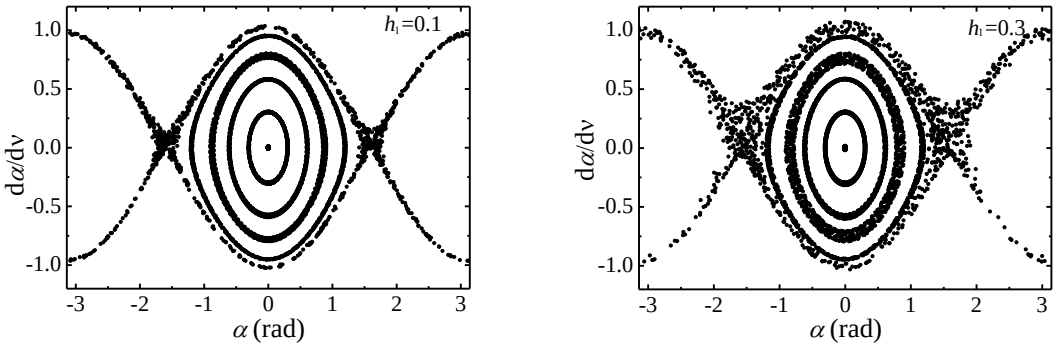


Figure 2. Poincaré map.

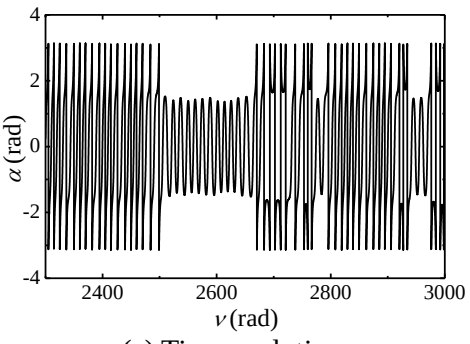


(a) Time evolution

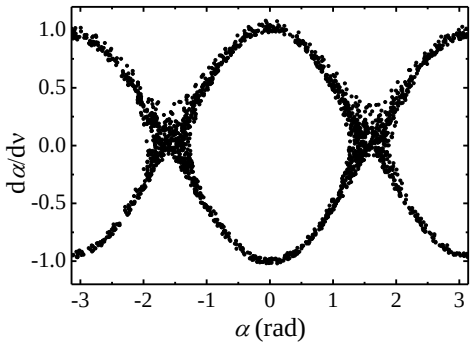


(b) Poincaré section, $\nu=2\pi$

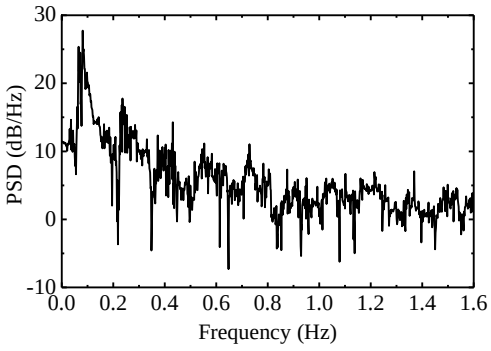


(c) Power spectrum density

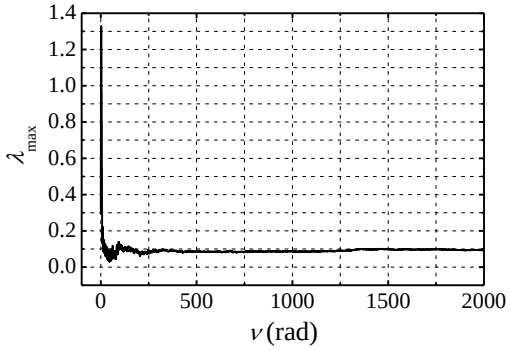


(d) The largest Lyapunov exponent

Figure 3. Chaotic motions by numerical calculations of the original system.

## 3. Dynamical equivalent model

The experimental system and its mechanics model for verifying the chaotic motion mentioned above is shown in figure 4, which consists of a marble table, a satellite simulator of the mass *m*, a dynamic measurement system, a communication system, and a power system. Four pressure-type solenoid valves and a momentum wheel were mounted on the simulator to yield the thrust forces $F_t$ and $F_r$ and the torque $M_z$, respectively.


Figure 4. The experimental system and its mechanics model.

The states of the satellite simulator are measured by a 3D-dynamic-measuring-system (DMS). The required thrust forces and the torque for simulating the Coriolis force and the on-orbit microgravity are computed by a host computer, according to a dynamical equivalent model. Meanwhile, they are sent back to the on-board computer on the simulator by wireless communication modules.

To implement the ground-based experiment, it is necessary to get a dynamical equivalent model for the on-orbital tethered satellite system. According to Lagrange's equations, the ground physical model shown in figure 4 obeys

$$\begin{cases} \ddot{\theta} = -\beta_1 \dot{\alpha}^2 \sin(\theta-\alpha) - \dfrac{F_r}{ml}\sin(\theta-\alpha) + (\dfrac{F_t}{ml} - \dfrac{\beta_1 M_z}{I_z})\cos(\theta-\alpha) \\ \ddot{\alpha} = \beta_2 \dot{\theta}^2 \sin(\theta-\alpha) + \dfrac{F_t \rho}{I_z}\sin^2(\theta-\alpha) + \dfrac{F_r \rho}{2I_z}\sin 2(\theta-\alpha) + \dfrac{M_z}{I_z} \end{cases} \tag{7}$$

where $\beta_1 = \rho/l$, $\beta_2 = m\rho l/I_z$. Here, the overdot represents the derivative with respect to the time *t*. By exerting the same torque to the mother satellite in figure 1 and converting equation (1) to the time scale, one can find a dynamically equivalency between equations. (1) and (7) by setting

$$\begin{cases} F_r = \dfrac{I_z}{\rho} B\cot(\theta-\alpha) - Aml\sin(\theta-\alpha) \\ F_t = \dfrac{I_z}{\rho} B + Aml\cos(\theta-\alpha) \\ M_z = -\beta_0 \dot{\nu}^2 I_z \sin\alpha\cos\alpha \end{cases} \tag{8}$$

with

$$\begin{cases} A = -\dfrac{3}{2}\dot{\nu}^2 \sin 2\theta - \beta_1[2\dot{\nu}\dot{\alpha}\sin(\theta-\alpha) + 3\dot{\nu}^2\cos\alpha\sin\theta] \\ B = \beta_2[2\dot{\nu}\dot{\theta} + 3\dot{\nu}^2\cos^2\theta]\sin(\theta-\alpha) \end{cases} \tag{9}$$

This means that the dynamics of the tethered satellite system arised from the Coriolis force and the microgravity can be demonstrated with the help of the thrust forces and the torque.

## 4. Experimental results

The mass of the satellite simulator was 12.2kg, the tether length and the offset distance were set at 0.88 and 0.01, respectively. The identified inertia moment of the simulator was 0.078kgm$^2$. Accordingly, the non-dimensional parameters were $\beta_0 = 3$, $\beta_1 = 0.0114$, and $\beta_2 = 1.376$. Given the true anomaly of on-orbit tethered satellite system is so small that resulting the equivalent thrust force is unable to push the simulator to move, due to the inevitable friction between the simulator and the marble platform. In order to match the experimental demand for the thrust forces, thus, the true anomaly used in the experiment was taken as $\dot{\nu} = 0.06$rad/s, according to the test on the thrust forces for true anomaly rates shown in figure 5. The corresponding thrust forces and the torque are displayed in figure 6 for the initial states $(\theta_0, \dot{\theta}_0, \alpha_0, \dot{\alpha}_0) = (0.1, 0, -0.1, 0)$.

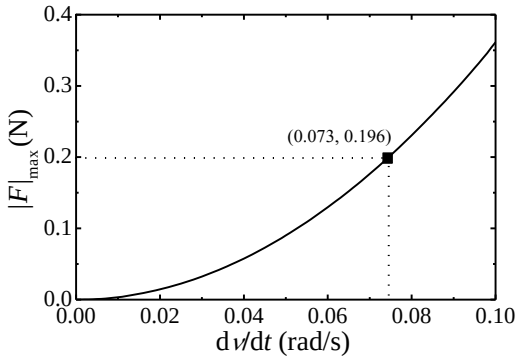


Figure 5. The maximum thrust force versus the true anomaly rate.

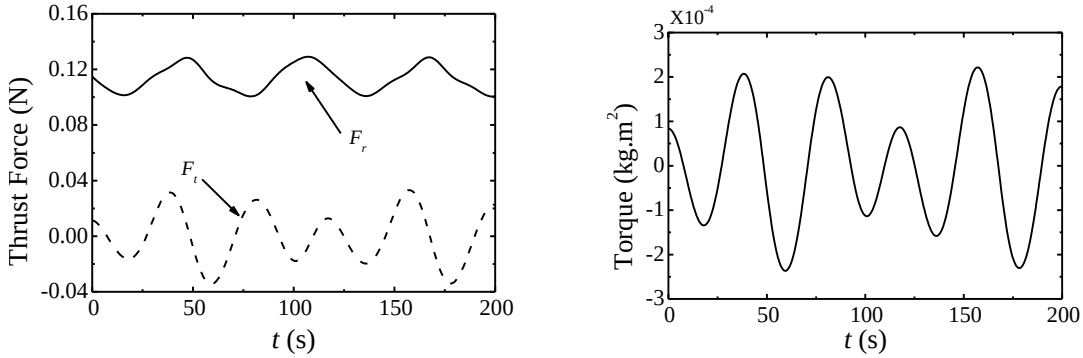


Figure 6. Time histories of the thrust forces and the torque.

The equivalent torque in equation (8) is not taken into account in experiment first. In this situation, the numerical and experimental results show that the motion of tether exhibits a regular harmonic oscillation as shown in figure 7. The attitude motion of mother is depictured in figure 8. One can see from figures 8(a) and 8(b) that an irregular oscillation occurs in the tethered satellite system. Furthermore, the continuous power spectrum and the positive largest Lyapunov exponent show that the irregular oscillation falls into a chaotic motion, as seen in figure 8(c) and 8(d). The experimental results suggest that chaotic motions and an irregular oscillation can co-exist in a tethered satellite system.

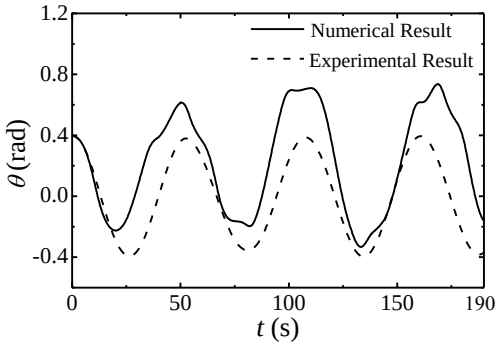


Figure 7. The motion of tether versus time for $(\theta_0, \dot{\theta}_0, \alpha_0, \dot{\alpha}_0) = (0.396, 0, -1.173, 0)$.

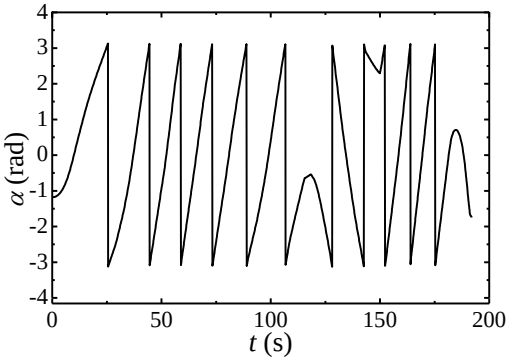


(a) Time evolution

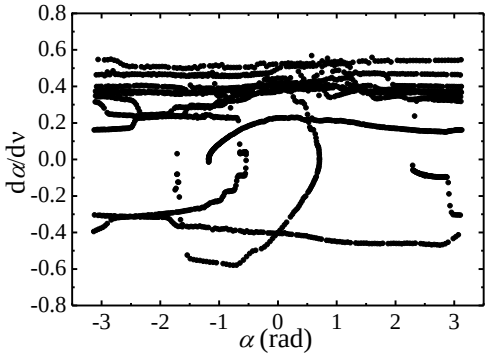


(b) Phase portrait

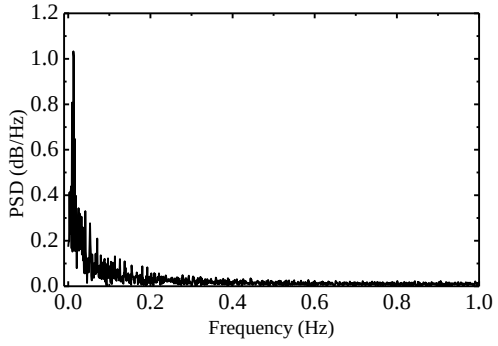


(c) Power spectrum density

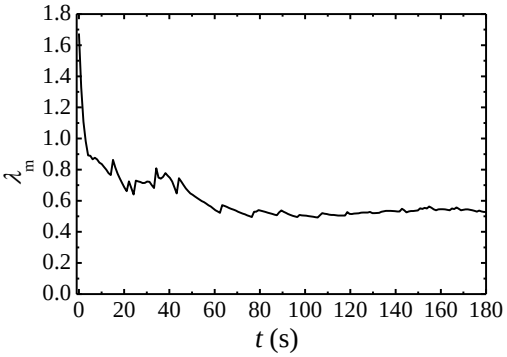


(d) The largest Lyapunov exponent

Figure 8. The attitude motion of mother for $(\theta_0, \dot{\theta}_0, \alpha_0, \dot{\alpha}_0) = (0.396, 0, -1.173, 0)$.

To suppress the chaotic motion of mother, a damping moment, $M_z = -kI_z\dot{\alpha}$, provided by the momentum wheel on the satellite simulator is put into the equivalent torque shown in equation (8), with the damping coefficient $k$=0.05. At the same way, the attitude motion of mother under the damping moment is obtained as shown in figure 9. According to the single peak of power spectrum and the negative Lyapunov exponent, it implies that the chaotic motion is guided to a regular oscillation near a relative equilibrium position. This means the chaotic motion is successfully suppressed via the negative damping moment.

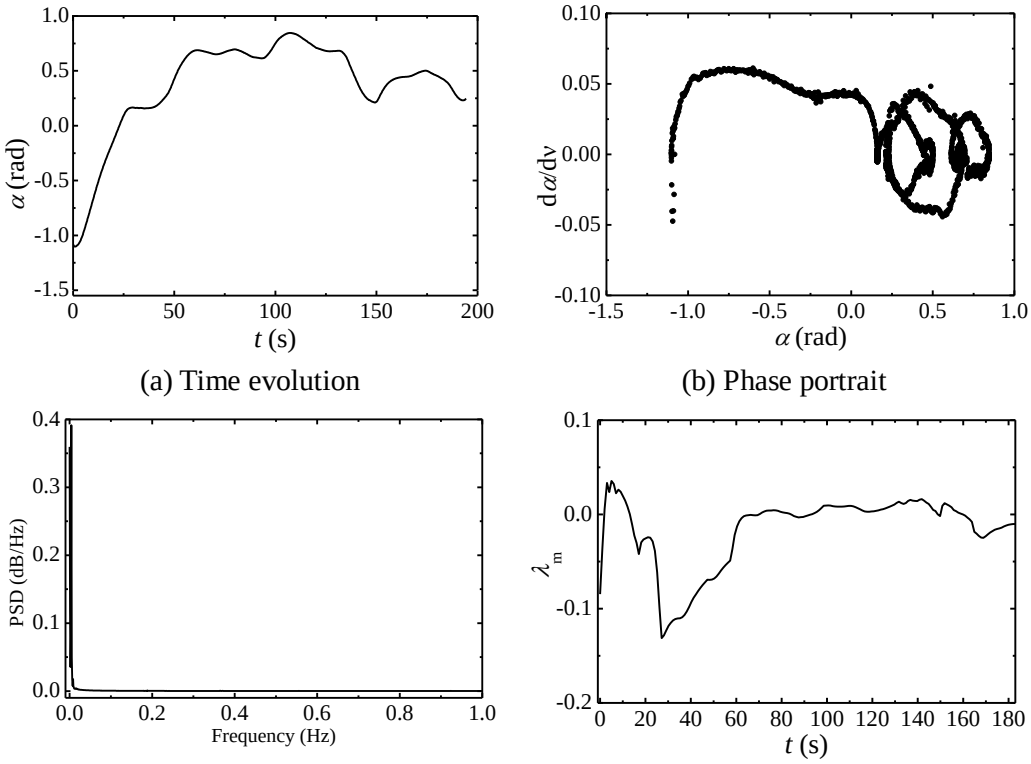


(a) Time evolution (b) Phase portrait

(c) Power spectrum density (d) The largest Lyapunov exponent

Fig. 9. The attitude motion under damping moment for $(\theta_0, \dot{\theta}_0, \alpha_0, \dot{\alpha}_0) = (0.398, 0, -1.08, 0)$.

## 5. Conclusions

The chaotic motion of tethered satellite system can be simulated by ground-based experimental system. The dynamical equivalent model between the on-orbit tethered satellite and its ground physical model can be obtained via dynamics similarity. So, the dynamics of on-orbit tethered satellite system arised by the Coriolis force and the on-orbit microgravity can be demonstrated in ground experiment. In addition, the experiment results show that the chaotic motion of mother is guided to a regular oscillation via the negative damping moment provided by the momentum wheel on satellite simulator.

**Acknowledgements**
This work was supported by the National Natural Science Foundation of China under Grants (11002068 and 11202094), and the Foundation for the Author of National Excellent Doctoral Dissertation of China (201233).

**References**

[1] Swan P A 1984 *Dynamics and control of tethers in elliptical orbits* (Ph.D. Dissertation: University of California)
[2] Jin D P, Wen H and Chen H 2013 Nonlinear resonance of a subsatellite on a short constant tether *Nonlinear Dynamics* **71** 479–88
[3] Aslanov V S and Ledkov A S 2012 Chaotic oscillations of spacecraft with an elastic radially oriented tether *Cosmic Research* **50** 188–98

[4] Pang Z J, Yu B S and Jin D P 2015 Chaotic motion analysis of a rigid spacecraft dragging a satellite by elastic tether *Acta Mechanica* **226** 2761–71
[5] Yu B S and Jin D P 2010 Deployment and retrieval of tethered satellite system under $J_2$ perturbation and heating effect *Acta Astronautica* **67** 845–53
[6] Wen H, Jin D P and Hu H Y 2008 Advances in dynamics and control of tethered satellite systems *Acta Mechanica sinica* **24** 229–41
[7] Nixon M S and Misra A K 1993 Nonlinear dynamics and chaos of two-body tethered satellite systems *Advances in the Astronautical Sciences* **85** 775–94
[8] Fujii H A and Ichiki W 1997 Nonlinear dynamics of the tethered subsatellite system in the station keeping phase *Journal of Guidance, Control, and Dynamics* **20** 403–06
[9] 9 Steiner W 1998 Transient chaotic oscillations of a tethered satellite system *Acta Mechanica* **127** 155–63
[10] Misra A K, Nixon M S and Modi V J 2001 Nonlinear dynamics of two-body tethered satellite systems: Constant length case *Journal of the Astronautical Sciences* **49** 219–36
[11] Chen H, Wen H, Jin D P and Hu H Y 2013 Experimental studies on tethered satellite systems *Advances in Mechanics* **43** 173–83 (in Chinese)
[12] Kojima H, Furukawa Y and Trivailo P M 2011 Experimental verification of periodic libration of tethered satellite system in elliptic orbit *Journal of Guidance, Control, and Dynamics* **34** 614–18